13th International Conference on
Structural Health Monitoring of Intelligent Infrastructure
DOI: 10.3217/978-3-99161-057-1-069

# Identification of Damping Coefficients of Multi-degree of Freedom System

Mohammad Shamim Miah[1, (0000-0001-9112-4049)], Werner Lienhart[1, (0000-0002-2523-4052)]
[1]Institute of Engineering Geodesy and Measurement Systems, Faculty of Mathematics, Physics and Geodesy, Graz University of Technology, Steyrergasse 30, 8010 Graz, Austria
email: miah@tugraz.at, werner.lienhart@tugraz.at

ABSTRACT: Structural dynamical properties are vulnerable to the dynamic loads because such loads can change those parameters significantly. It is not possible to halt the aforementioned issue as dynamic loads are entirely unpredictable. The changes in stiffness, mass, and damping can lead to minor to serious damage scenarios depending on the level of changes of those parameters. Typically, the displacements trajectories of any systems are unknown, and if any other physical parameters e.g. damping is unknown that will form a nonlinear problem. Herein, to deal with the early mentioned problem a nonlinear observer namely the unscented Kalman filter (UKF) is employed. In conventional practice, the partial or full stiffness matrix are identified but identifying damping matrix is rare due to inherent complicacy. Hence, this study has focused on the identification of the entire damping matrix by adopting the UKF. The outcome of study shows that UKF is capable of identifying damping coefficients quite accurately. This outcome can play a vital role in the area of structural health monitoring and control applications.

KEY WORDS: Structural Health Monitoring, Unscented Kalman Filter, Dynamic Loads, Damage.

## 1 INTRODUCTION

System identification is a process that helps to estimate any desire quantities e.g. stiffness based on measured sensory data and develop an underlying mathematical model of the dynamical system. Typically, the goal of the system identification is to develop a representative model that can render the true behavior of the dynamical system. Modern structures are getting complicated to monitor due to many underlying uncertainties such as their form, adaptation of state-of-art technologies e.g. sensors, dampers, monitoring tools. Therefore, monitoring such structures require proper tools, scheme and knowledge to deal with hidden uncertainties. For instance, in order to keep track on any changes real-time monitoring could be an option [1], [5], [13] and [14]. On the other hand, system identification might assist to understand the structure better as it might help to update the virtual or mathematical systems real-time or offline.

System identification (SI) is a shared topic in many areas of science and engineering e.g. mechanical/civil engineering, robotics, process engineering [15][16]. However, in case of civil engineering application still the use and application of SI is limited due to associated problems, for instance, models are very large compare to a robot or mechanical tool. Dealing with large model require serious attention as many variables are unknows along with inputs. To deal with the numerous uncertainties, typically, from the measured data, stiffnesses are identified and feed to the control loop to adjust and update the model. Thereby, the updated model can render the true system behavior better contrary to doing no update. If the aforementioned process is done in real-time, optimal control performances can be expected.

Many works can be found those who tried various methods to identify different parameters of various type of structures e.g. buildings, bridges. Among them, a new type black-box by the use of extended Kalman filter (EKF) is studied for SI [4], a neural network and dead-zone Kalman filter algorithm has been reported in [6], SI for time-varying system [7], autoregressive models based frequencies and damping ratio identification by [8], new forms of EKF for SI [9], SI for medical image processing application [10], SI using stochastic filter techniques [12]. The fundamental concept of the Kalman filter was proposed by Rudolf E. Kalman in 1960 [17]. Later, many have been proposed and developed different nonlinear filters such as EKF and UKF [11], [18] and [19] and their modified version.

It is mentioned early that stiffness are often identified for civil engineering application due to the simplicity in contrast to identifying damping. For instance, a detail theoretical formulation and an experimental validation of semi-active control problem along with stiffness matrix identification has been carried out in [14]. In the aforementioned study, author did not perform the identification of damping matrix individually or linked to any control problem. Because, damping coefficients are extremely sensitive to inputs and material properties as a result dealing with the control problem makes things troublesome or even could lead to an uncontrollable situation. Therefore, not many studies have been conducted in case of damping coefficients/matrices in combination with states due to the underlying complicacy. More specifically, when both sates and damping coefficients are unknown simultaneously, it leads to a nonlinear problem that requires a nonlinear observer to solve. The aforementioned problem has been focused in [20] to identify damping matrix where main consideration was to see the effect of initial covariance of the observer. Another work [3] has tried to identify damping via sensitivity enhanced method linked to Principal Component Analysis. A more detail issues linked to nonlinear damping identification has been reported in [2].

From above discussion it is clear that identification of damping itself leads to a complicated problem and it gets more

DOI: 10.3217/978-3-99161-057-1-069

complicated when both sates and damping coefficients are unknown. To handle this issue, this study has focused into the identification of damping coefficients along with unknown states. A 15 degree-of-freedom (DOF) dynamical system is consider for the numerical implementations. The system identification task is performed by employing the unscented Kalman filter (UKF). The overall outcome shows that the UKF is capable of identifying damping coefficients quite accurately. As a result, the dynamical response (e.g. displacements) of the system shows excellent match with the response of the true system. Rest of the paper contains, problem description & formulation, results and discussion and finally a summary of the study.

## 2 PROBLEM DESCRIPTION & FORMULATION

The numerical investigations are conducted by adopting a 15 storied dynamical system. The dynamical system is considered to be model as lumped-mass-spring system as depicted in Figure 1. A sample free-body diagram of the top floor and a typical floor is shown in the early mentioned figure along with the full structure. Typically, equation of motion (EOM) is derived for each floor from the free-body diagram of the structure. As for example, an EOM has been derived for the 1st DOF as shown below,

$$m_1\ddot{x}_1(t) + c_1\dot{x}_1(t) + k_1x_1(t) - c_1[\dot{x}_2(t) - \dot{x}_1(t)] - k_1[x_2(t) - x_1(t)] = -\ddot{u}_1(t) \quad (1)$$

$$m_1\ddot{x}_1(t) + [c_1 + c_2]\dot{x}_1(t) - c_1\dot{x}_2(t) + [k_1 + k_2]x_1(t) - k_1x_2(t) = -\ddot{u}_1(t) \quad (2)$$

Later, all those equations of motion are combined into one single equation in matrix-vector form. And the dynamical model can be expressed in vector-matrix form as,

$$M\ddot{X}(t) + C\dot{X}(t) + KX(t) = -\beta\ddot{u}_g(t) \quad (3)$$

where M, C and K are the mass, damping and stiffness matrices with a size of $15 \times 15$, $X$, $\dot{X}$ and $\ddot{X}$ are the displacement, velocity, and acceleration vector those have a size of $15 \times 1$, $\ddot{u}_g$ is the input excitation, $\beta$ controls input excitations location, $t$ is the time vector.

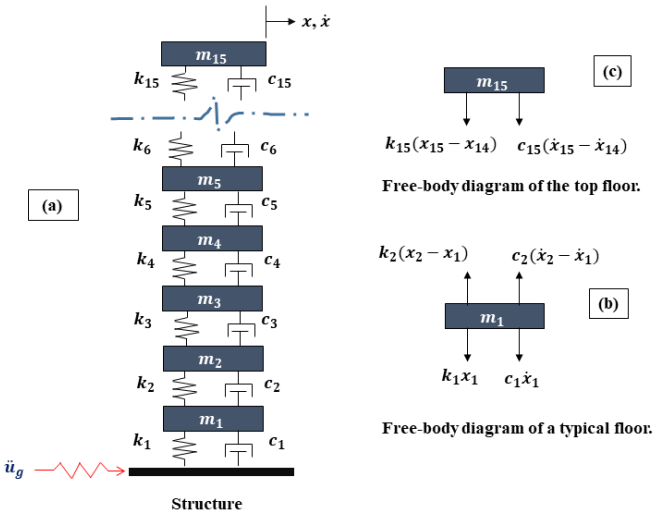


Figure 1. The structure and sample free-body diagram of a typical floor and top floor.

It is quite common that the dynamical system further formulated by adopting the state space (SS) formulation technique. The SS formulation contains two main equations, they called, (i) the process equation in Eq. (2), and (ii) the observation equation in Eq. (3).

$$x_{k+1} = Ax_k + Bu_k \quad (4)$$

$$y_k = Cx_k + Du_k \quad (5)$$

where $x$ is the states vector that has displacement and velocity, $A$ is the state matrix, $B$ represents the input matrix, it can be with single of multi inputs, $D$ is the feedthrough matrix, $C$ is output matrix, $u$ contains input and control force (if any), $y$ is the output vector.

Step ahead, the noise terms (both process and observation) are added to the SS formulation to deal with the observer. Typical, formulation of the UKF would look like,

$$x_{k+1} = f(x_k, v_k) \quad (6)$$

$$y_k = h(x_k, n_k) \quad (7)$$

where $v_k$ represent process noise and $n_k$ is the observation noise. The dynamical systems are described via $f$ and $h$ functions [18]-[19]. UKF propagates random variables using a specific statistical procedure known as the unscented transformation (UT). Due the aforementioned procedure UKF is derivative free, as a result it is faster than its counterpart EKF [18]. In short, a structured transformation, distributed equally around the mean (also known as the sigma points) that propagate through early mentioned complex nonlinear functions. The sigma points ($\hat{x}_k$) are estimated as follows, $\hat{x}_k = \left[\hat{x}_{k-1}\ ,\ \hat{x}_{k-1} + \sqrt{(L+\lambda)P_{k-1}}\ ,\ \hat{x}_{k-1} - \sqrt{(L+\lambda)P_{k-1}}\right]$, where $L$ is the dimension of the states and $\lambda$ is a scaling factor. There are two main steps for the UKF, they are known as (i) the prediction Eq. (6) and (ii) the measurement update Eq. (7).

$$\hat{x}_{k|k-1} = f(\hat{x}_{k-1}, u_{k-1}) + w_{k-1} \quad (8)$$

$$\hat{y}_{k|k-1} = h\left(\hat{x}_{k|k-1}\right) + v_k \quad (9)$$

A simplified flow-chart of the UKF is depicted in Figure 2. The overall estimation is done recursively until the simulation ends.

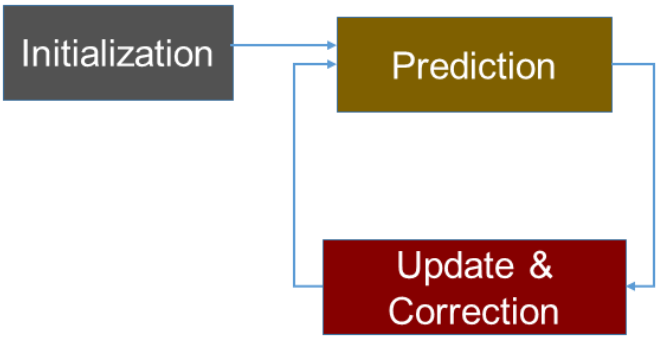


Figure 2. Basic steps of the UKF.

The estimation steps of the UKF is given below with more detail:

DOI: 10.3217/978-3-99161-057-1-069

(i) The initialization step (setting the states and covariance):

$$\hat{x}_0 = E[x_0], P_0 = E[(x_0 - \hat{x}_0)(x_0 - \hat{x}_0)^T]$$

$$\hat{x}_0^a = E[x^a] = [\hat{x}_0^a \; 0 \; 0]^T, P_0^a = E[(x_0^a - \hat{x}_0^a)(x_0^a - \hat{x}_0^a)^T]$$

(ii) The Sigma Points estimation:

$$\gamma_{k-1}^a = \left[\hat{x}_{k-1}^a \,,\, \hat{x}_{k-1}^a + \sqrt{(L+\lambda)P_{k-1}^a} \,,\, \hat{x}_{k-1}^a - \sqrt{(L+\lambda)P_{k-1}^a}\right]$$

(iii) The prediction or time update:

$$\gamma_{k|k-1}^x = f[\gamma_{k-1}^x \,,\, \gamma_{k-1}^v]$$

$$\hat{x}_k^- = \sum_{i=0}^{2L}\left[w_i^m \gamma_{i,k|k-1}^x\right]$$

$$P_k^- = \sum_{i=0}^{2L}\left[w_i^c\left(\gamma_{k|k-1}^x - \hat{x}_k^-\right)\left(\gamma_{k|k-1}^x - \hat{x}_k^-\right)^T\right]$$

$$\tau_{k|k-1} = h\left[\gamma_{k|k-1}^x \,,\, \gamma_{k|k-1}^n\right]$$

$$\hat{y}_k^- = \sum_{i=0}^{2L}\left[w_i^m \tau_{i,k|k-1}\right]$$

(iii) The measurement update & correction:

$$P_{\bar{y}_k\bar{y}_k} = \sum_{i=0}^{2L}\left[w_i^c\left(\tau_{i,k|k-1} - \hat{y}_k^-\right)\left(\tau_{i,k|k-1} - \hat{y}_k^-\right)^T\right]$$

$$P_{x_k y_k} = \sum_{i=0}^{2L}\left[w_i^c\left(\gamma_{i,k|k-1} - \hat{x}_k^-\right)\left(\tau_{i,k|k-1} - \hat{y}_k^-\right)^T\right]$$

$$\hat{x}_k = \hat{x}_k^- + P_{x_k y_k} P_{\bar{y}_k\bar{y}_k}^{-1}[y_k - \hat{y}_k^-]$$

where $P_x$ is the process noise covariance, $P_y$ is the measurement noise covariance, $w_i$ is the weight parameters [462].

## 3 RESULTS AND DISCUSSION

The numerical investigations are conducted by adopting a 15 degree of freedom (DOF) dynamical system. Therefore, the mass, damping and stiffness matrices size are $15 \times 15$, while, the mass matrix is assumed to be fully-diagonal. The mass is assumed to be equal in each floor and the weight of every floor is around $60 \times 10^3$ Kg. And the stiffness components of each floor are considered $65 \times 10^5$ N/m. The damping coefficients are estimated using eigenfrequencies and a damping ration of 2%. The main goal here is to identify all of the 15 damping coefficients. To do this, UKF is employed as nonlinear observer and the numerical investigations are conducted for 160 sec with a sampling rate of 200 Hz. The harmonic type input excitation ($\ddot{a}_g = 1 \times \sin(16.5t)$) is used to excite the structure (see Figure 3). The harmonic type input load has been selected due to the simplicity of the nature of the load in contrary to complex type input e.g. earthquake.

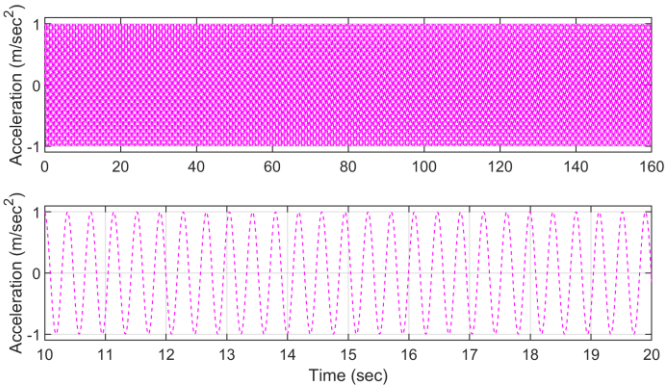


Figure 3. Input excitation: full-time series (top), zoomed view (bottom).

The comparison of the original versus identified damping coefficients are presented in Figure 4, Figure 5, and Figure 6. More precisely, the damping coefficients are separated as $c_1 - c_5$ in Figure 4, $c_6 - c_{10}$ in Figure 5, and $c_{11} - c_{15}$ in Figure 6, respectively. The aforementioned separation is done for better visualization purpose. Additionally, the values are normalized with respect to the top floor's value for the same reason as mentioned earlier.

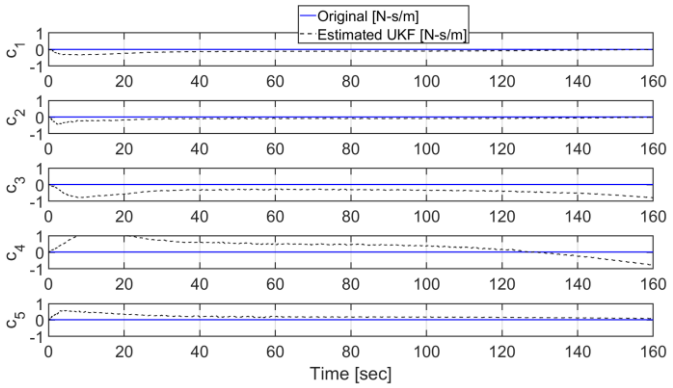


Figure 4. Comparison of the original and identified damping coefficients $[c_1 - c_5]$.

It is observed that the accuracy of the estimated damping coefficients is in generally good. However, few parameters have struggled than their peers, it is due to the size of model's variables, meaning, more parameters lead to complex tuning process (e.g. noise level, initial covariances, etc.), similar issues have been reported by many [12], [20] and [21]. However, even after hard tuning still at the end accuracy may not be as expected because it is mentioned earlier that the accuracy is not depended on any single variable.

DOI: 10.3217/978-3-99161-057-1-069

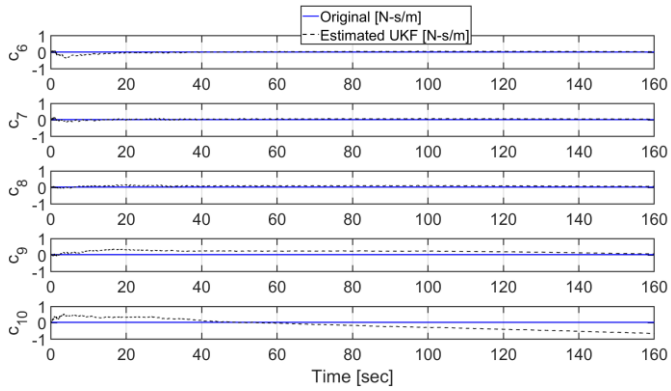


Figure 5. Comparison of the original and identified damping coefficients $[c_6 - c_{10}]$.

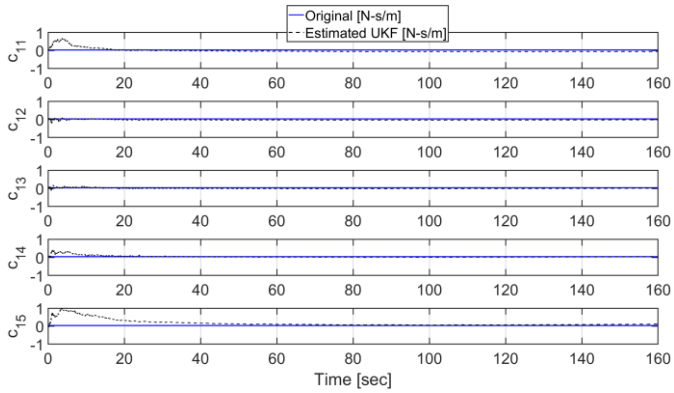


Figure 6. Comparison of the original and identified damping coefficients $[c_{11} - c_{15}]$.

There are many underlying uncertainties for parameters identification in general and it gets worse when it comes to damping. It is due to the nature of the damping itself and there are many influencing factors such as amplitudes of the inputs, initial covariances and noise. Additionally, the accuracy of the estimation/identification may change significantly if the sampling rate, duration of the simulation, initial states and covariances are not tuned properly. A summary of the identified damping coefficients is given in Table 1. Along with the early mentioned table a graphical representation of the data is shown in Figure 7. It should be noted that the normalized errors are estimated based on the last value at the end of the simulation. Hence for better understanding, Figure 4, Figure 5, and Figure 6 are recommended to see the whole time-series. As the parameters take some time to reach in stable or so-called steady-state condition hence errors are not isolation to a point of time of simulation (for example the identified value in the table).

Table 2. Summary of the identified damping coefficients.

| Damping coefficients | Original | Identified* | Normalized Error (%) |
|---|---|---|---|
| $c_1$ | 1273.55 | 1665.95 | 0.016 |
| $c_2$ | 3807.57 | 5017.11 | 0.048 |
| $c_3$ | 6302.52 | 501131.164 | 19.78 |
| $c_4$ | 8732.81 | 493153.22 | 19.36 |
| $c_5$ | 11073.48 | 53097.78 | 1.68 |
| $c_6$ | 13300.52 | 25630.01 | 0.49 |
| $c_7$ | 15391.08 | 28422.90 | 0.52 |
| $c_8$ | 17323.71 | 47258.82 | 1.19 |
| $c_9$ | 19078.57 | 42974.68 | 0.95 |
| $c_{10}$ | 20637.66 | 411245.85 | 15.61 |
| $c_{11}$ | 21984.98 | 36596.87 | 0.58 |
| $c_{12}$ | 23106.76 | 3977.92 | 0.76 |
| $c_{13}$ | 23991.326 | 7640.00 | 0.65 |
| $c_{14}$ | 24629.76 | 28217.52 | 0.14 |
| $c_{15}$ | 25015.46 | 75434.76 | 2.01 |

*absolute identified values belong to the end of the simulation

Further, the propagation of the uncertainties have evaluated and given as the root mean squared (RMS) and the standard deviations (STD), those values are estimated and illustrated in Figure 8 and Figure 9, respectively. Both the RMS values and STD shows that they are not constant and consistent throughout the simulation period. That also justify why the identified parameters may have different level of errors based-on at what point the parameters are considered.

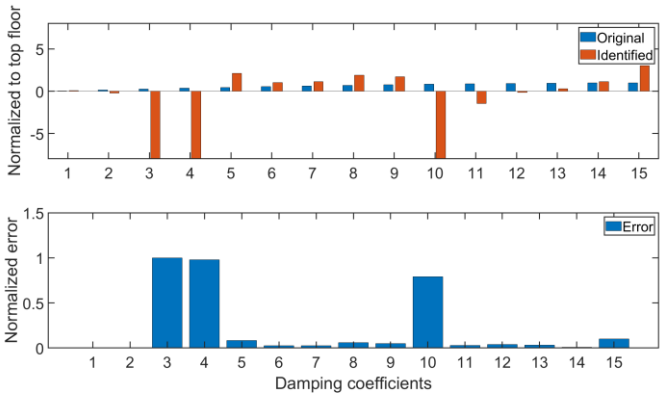


Figure 7. Comparison of the original and identified damping coefficients and their errors $[c_1 - c_{15}]$.

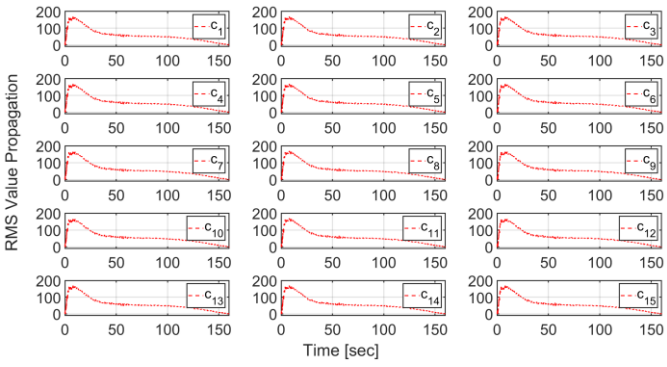


Figure 8. Point-to-point error changes during the simulation period $[c_1 - c_{15}]$.

DOI: 10.3217/978-3-99161-057-1-069

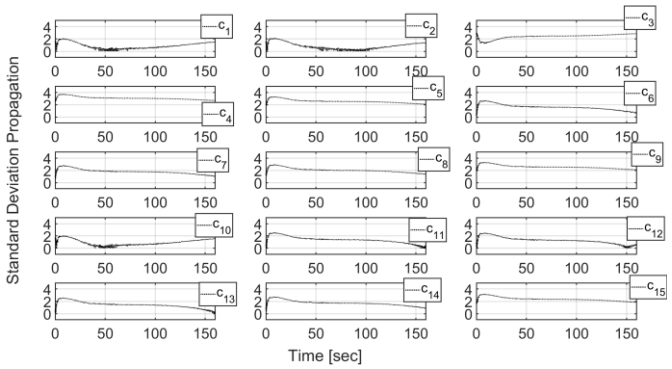


Figure 9. Standard deviation changes during the simulation period $[c_1 - c_{15}]$.

Furthermore, to understand the effect of the identified damping coefficients, the displacements trajectories of the 5th, 10th and 15th DOF is evaluated. The displacement of 5th floor is depicted in Figure 10, while Figure 11 has the 10th floor displacement and the 15th floor displacement is shown in Figure 12. All of the aforementioned figures have a full-time series (top sub figure) and a zoomed view (bottom sub figure). It can be observed that all of those figures show a very good accuracy in terms of rendering the original behavior of the system.

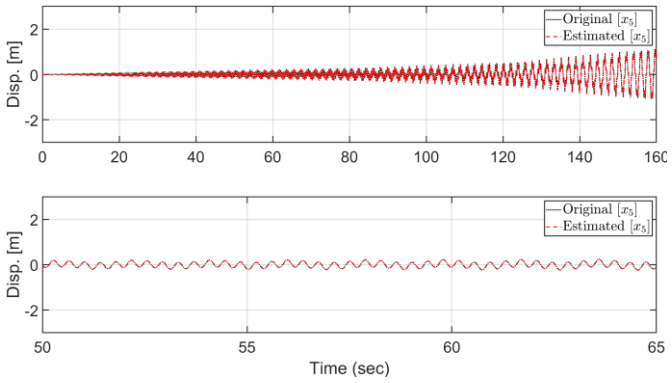


Figure 10. Original versus estimated displacement of the 5th floor.

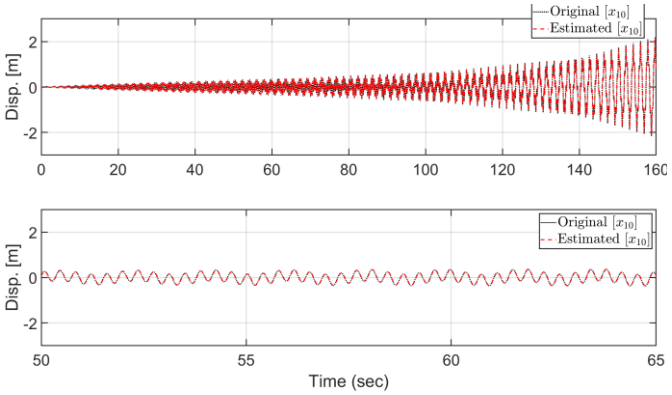


Figure 11. Original versus estimated displacement of the 10th floor.

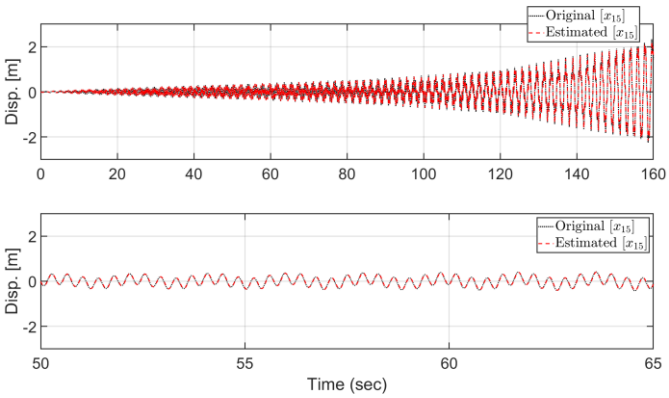


Figure 12. Original versus estimated displacement of the 15th floor.

Last but not least, the acceleration response of those early mentioned floors (e.g. 5th, 10th and 15th) has been evaluated and presented in Figure 13, Figure 14, and Figure 15, correspondingly. Similar to the earlier observation, it has been noticed that the estimated acceleration data render the original data quite accurately.

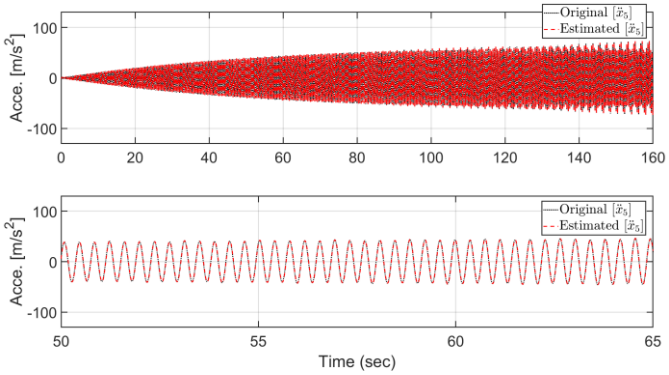


Figure 13. Original versus estimated acceleration of the 5th floor.

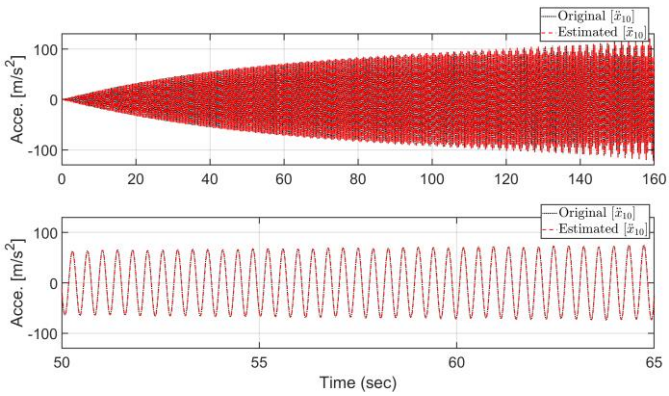


Figure 14. Original versus estimated acceleration of the 10th floor.

DOI: 10.3217/978-3-99161-057-1-069

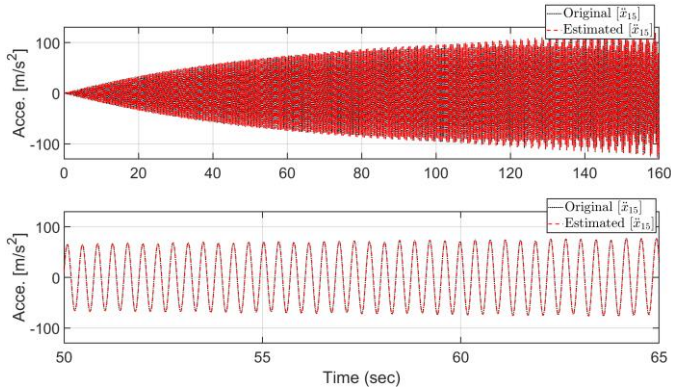


Figure 15. Original versus estimated acceleration of the top floor.

## 4 CONCLUSION

This study investigates the possibility of identification full damping matrix of a 15 DOF system. The goal is achieved by adopting the UKF as an observer. The estimated parameter results show very good match with the original data. The displacement and acceleration comparison results confirm (due to their a very good match) that the identified damping coefficient are quite accurate. However, that doesn't mean that all 15 damping coefficients (e.g. $c_1 - c_{15}$) are having same accuracy. UKF perform recursive estimation during the given time-span hence the error of the estimation is optimized by minimizing errors. In other words, the accuracy of the states (displacements and velocities) are not very much affected due to the individual damping coefficient accuracy. In a nutshell, the outcome of this study can be summarized that the investigated approach might be beneficial for structural health monitoring and vibration control applications as the states can be updated during the simulation in real-time.

## ACKNOWLEDGMENTS

Authors appreciate the research supports and facilities provided by the Graz University of Technology, Graz, Austria.

## REFERENCES

[1] Z. Xie and J. Feng, Real-time nonlinear structural system identification via iterated unscented Kalman filter, Mechanical Systems and Signal Processing, 28, 309–322, 2012.
[2] T. Al-Hababi, M. Cao, B. Saleh, N. F. Alkayem and H. Xu, A critical review of nonlinear damping identification in structural dynamics: Methods, applications, and challenges. Sensors (Switzerland), 20(24), 1-41, 2020.
[3] X. Wang, K. Liu, H. Liu and Y. He, Damping Identification with Acceleration Measurements Based on Sensitivity Enhancement Method. Shock and Vibration, 2018, 6476783, 2018.
[4] K. Bogdanski and M. C. Best, A new structure for non-linear black-box system identification using the extended Kalman filter. Proceedings of the Institution of Mechanical Engineers, Part D: Journal of Automobile Engineering, 231(14), 2005-2015, 2017.
[5] M. Wu and A. W. Smyth, Application of the unscented Kalman filter for real-time nonlinear structural system identification. Structural Control and Health Monitoring, 14(December 2005), 971–990, 2007.
[6] J. Dejesusrubio and W. Yu, Nonlinear system identification with recurrent neural networks and dead-zone Kalman filter algorithm. Neurocomputing, 70(13–15), 2460–2466, 2007.
[7] B. Weng and K. E. Barner, Time-Varying Volterra System Identification Using Kalman Filtering. Information Sciences and Systems, 2006 40th, 1617–1622, 2006.
[8] H. Kosorus, M. Hollrigl-Binder, H. Allmer and J. Kung, On the Identification of Frequencies and Damping Ratios for Structural Health Monitoring Using Autoregressive Models. 2012 23rd International Workshop on Database and Expert Systems Applications, 23–27, 2012.
[9] S. Ghosh, D. Roy and C. Manohar, New forms of extended Kalman filter via transversal linearization and applications to structural system identification. Computer Methods in Applied Mechanics and Engineering, 196(49–52), 5063–5083, 2007.
[10] J. Yin and V. Syrmos, System identification using the extended Kalman filter with applications to medical imaging. American Control Conference, June, 2000.
[11] L. Jeen-Shang and Z. Yigong, Nonlinear structural identification using extended Kalman filter. Computers and Structures, 52(4), 757–764, 1994.
[12] C. Myungjin and T. Sato, Structural Identification using Stochastic Filtering Techniques Based on Measurements from Wireless Data Acquisition System. Steel Structures, 6, 353–360, 2006.
[13] M. S. Miah, E. N. Chatzi, V. K. Dertimanis and F. Weber, Real-time experimental validation of a novel semi-active control scheme for vibration mitigation. Structural Control and Health Monitoring, 24(3), e1878, 2017.
[14] M. S. Miah, Semi-Active Control for Magnetorheological Dampers via Coupling of System Identification Methods. ETH-Zürich, 22776, 1–137, 2015.
[15] L. Ljung, System Identification: Theory for the User. Second edition. PTR Prentice Hall, Upper Saddle River, NJ, 1999.
[16] van Overschee, P., and B. De Moor. Subspace Identification of Linear Systems: Theory, Implementation, Applications. Springer Publishing: 1996.
[17] R. E. Kalman, A new approach to linear filtering and prediction problems. Journal of Basic Engineering, 82(Series D), 35–45, 1960.
[18] S. J. Julier and J. K. Uhlmann, A New Extension of the Kalman Filter to Nonlinear Systems. Int. Symp. Aerospace/Defense Sensing, Simul. and Controls, 3, 1–12, 1997.
[19] E. Wan and R. Van Der, Merwe, The unscented Kalman filter. In S. Haykin (Ed.), Kalman filtering and neural Network, John Wiley and Sons, Inc, 5, 221–280, 2001.
[20] M. S. Miah, M. Kaliske and M. J. Miah, Damping Matrix Identification for Structural Health Monitoring Considering Sensitivity of Initial Unknown Covariance. Proceedings of the 4th World Congress on Civil, Structural, and Environmental Engineering (CSEE'19), 1–9, 2019.
[21] K. Xiong, H. Y. Zhang, and C. W. Chan, Performance evaluation of UKF-based nonlinear filtering. Automatica, 42(2), 261–270, 2006.